INTERNATIONAL JOURNAL OF CLIMATOLOGY
*Int. J. Climatol.* (2017)
Published online in Wiley Online Library
(wileyonlinelibrary.com) DOI: 10.1002/joc.5317

RMetS
Royal Meteorological Society

# Uncertainties of gridded precipitation observations in characterizing spatio-temporal drought and wetness over Vietnam

Tue M. Vu,[a,b]* Srivatsan V. Raghavan,[a,c,d] Shie-Yui Liong[a,c,d,e] and Ashok K. Mishra[b]

[a] *Tropical Marine Science Institute, National University of Singapore, Singapore*
[b] *Glenn Department of Civil Engineering, Clemson University, SC, USA*
[c] *Department of Civil and Environmental Engineering, Center for Hazards Research, National University of Singapore, Singapore*
[d] *Center for Environmental Sensing and Modeling, Singapore-MIT Alliance for Research and Technology Centre, Singapore*
[e] *Willis Re Inc., London, UK*

**ABSTRACT:** Precipitation is an important climate variable to investigate extreme events (e.g. drought and flood) as well as to develop robust strategies for water resources planning and management. Lack of adequate and robust information on precipitation poses great difficulties in understanding the observed climate as well as to validate climate model outputs. To overcome this limitation gridded precipitation data sets have been constructed to supplement the lack of *in situ* data. This study compares five popular gridded precipitation data sets to evaluate their performance in terms of drought and wetness over Vietnam. These five gridded data sets include: (1) Asian Precipitation Highly Resolved Observational Data Integration Towards the Evaluation of Water Resources (APHRODITE), (2) Climate Precipitation Center (CPC), (3) Climate Research Unit (CRU), (4) Global Precipitation Climatology Center (GPCC) and (5) University of Delaware (UDEL). The recently developed gridded precipitation observational data 'VnGP' from Vietnam is used as the reference data set to assess the performance of these five gridded precipitation products. The Standardized Precipitation Index (SPI) is used to quantify drought and wetness. GPCC and APHRODITE performed reasonably well in reproducing spatial and temporal precipitation patterns. GPCC performs consistently better than APHRODITE in all the statistical tests. Except for UDEL, other gridded data sets able to exhibit the characteristics of drought/wetness (e.g. the percentage of drought events and severity) during strong El Nino Southern Oscillation (ENSO) events. However, higher uncertainty exists to quantify drought inter-arrival time in most of the data sets. Furthermore, trend analysis was performed to evaluate the comparative performance of gridded data sets to quantify drought (wet) spells at annual and seasonal time scales. Although the gauge-based and hybrid satellite–gauge merged products use partly ground truth data, the different interpolation techniques and merging algorithms may contribute to large uncertainties.

KEY WORDS uncertainty; gridded data sets; drought and wetness; Vietnam

*Received 30 May 2017; Revised 13 September 2017; Accepted 18 September 2017*

## 1. Introduction

The uncertainties between available gridded data sets and local rain gauge data can potentially influence water resources planning. These uncertainties can be attributed to sparse network observations, complex terrains, interrupted/limited in data monitoring records, instrument errors and especially for developing countries due to technology, financial issues and war time. Recent reviews have noted a marked decline in the amount of *in situ* data being collected in many parts of the world (Mishra and Coulibaly, 2009). Therefore, quantification of these data sets becomes necessary for use in local-scale water resources management. These data sets are also used for benchmarking global/regional climate models over areas with limited or missing data records or for use in impact analysis for floods and droughts. Gridded observation data are used to characterize spatio-temporal droughts and as well as for water resources management (Mishra and Singh, 2010; Vicente-Serrano *et al.*, 2012, 2014). Excessive drought and wetness affect natural habitats and ecosystems, economic and social sectors that include agriculture, transportation, urban water supply and other modern complex industries (Heim, 2002; Vu *et al.*, 2015). Regional drought leads to global impact on food supplies due to reduction in crop yields (Ciais *et al.*, 2005; Zhang and Zhou, 2015), undermines the economics and stability of governments (Sternberg, 2011) and regional wetness has severe implications on excessive flooding as well as flood risk management (Seiler *et al.*, 2002; Van Steenbergen and Willems, 2014).

There are several drought indices useful for monitoring drought/wetness indicators (Mishra and Singh, 2010): Palmer Drought Severity Index (PDSI) (Palmer, 1965), Standardized Precipitation Evapotranspiration

* Correspondence to: T. M. Vu, Glenn Department of Civil Engineering, Clemson University, Clemson, SC 29634, USA. E-mail: tuev@g.clemson.edu

Index (SPEI) (Vicente-Serrano *et al.*, 2010), Standardized Runoff Index (SRI) (Shukla and Wood, 2008) or, for precipitation only, Standardized Precipitation Index (SPI) (McKee *et al.*, 1993). In this study, the SPI is chosen for drought and wetness assessment because (1) we only focus on investigating the gridded precipitation (which is the only required variable used for deriving SPI) and (2) non-availability of enough *in situ* temperature/evapotranspiration/soil moisture data for the country. In addition, SPI is a popular index to characterize drought and wetness over many regions (Mishra and Singh, 2010).

There are several applications of gridded precipitation data sets for drought and wetness studies over the region. For example, Vu and Mishra (2016) derived SPI using Asian Precipitation Highly Resolved Observational Data Integration Towards the Evaluation of Water Resources (APHRODITE) data set to characterize drought and wetness condition over the Indochina Peninsula. Using outputs from a regional climate model, Vu *et al.* (2015) investigated drought (using SPI) over a region in the Central Highland of Vietnam and compared with gridded data sets. This study aims to investigate the uncertainties in using gridded precipitation data sets for monitoring drought and wetness over Vietnam. The satellite products were not evaluated in this study due to the nature of relatively shorter temporal records that do not capture some of the extreme historical drought/wetness events. The study comes in the backdrop of both having poor data coverage over Vietnam, especially spanning for remote areas and the need for a denser and robust network of observations that could also be used in real time to monitor local drought/wetness. Such assessments are crucial for the Vietnamese agricultural and water resources management sector. The country, being so vulnerable to floods and droughts and in general, natural disasters, receives less attention in the area of climate sciences, vulnerability and impact assessments.

## 2. Study region, data and methodology

Vietnam has a very sparse network of meteorological stations and more than 70% of the people depend on agriculture for their livelihood. Drought events are frequent and it has a wide range of impacts on agricultural and water resources sector. According to a drought assessment report by the Ministry of Agriculture and Rural Development (MARD), the major drought occurred during 1997–1998 (one of the strongest El Nino years) and about 3 million people were affected and the total losses in terms of agricultural production were estimated to be about 400 million US dollars.

### 2.1. Precipitation data sets

An overview of these selected gridded data sets is provided in Table 1. Because of the inconsistency in data length, the analysis is performed using a common time period 1980–2007. Brief descriptions of individual data sets are provided here.

Table 1. Gridded precipitation products used in the study.

| Name | Temporal resolution | Spatial resolution (°) | Source | Period |
|---|---|---|---|---|
| VnGP | Daily | 0.25 | Vietnam | 1980–2010 |
| APH | Daily | 0.25 | Japan | 1961–2007 |
| CPC | Monthly | 0.5 | USA | 1961–2007 |
| CRU | Monthly | 0.5 | UK | 1901–2015 |
| GPCC | Monthly | 0.5 | Germany | 1901–2013 |
| UDEL | Monthly | 0.5 | USA | 1901–2014 |

#### *2.1.1. Vietnam-gridded precipitation data*

The most recent Vietnam-gridded precipitation data (VnGP) were constructed using 481 rain gauges over Vietnam (Nguyen *et al.*, 2016). It was noted that among multiple interpolations tested, the Spheremap interpolation technique showed relatively better performance compared to the other methods such as the inversed distance weighting, Kriging and Cressman methods and was therefore chosen to construct the VnGP. These data sets are available at daily time scale in two different spatial resolutions (0.25 and 0.1°) for the time period 1980–2010. The study by Nguyen *et al.* (2016) has validated VnGP with gauge observation in terms of spatial distribution, correlation, mean absolute error, root-mean-square error and obtained good results. To our knowledge, the VnGP is the best precipitation observation gridded data set that is currently a good representation of gauge observations over Vietnam. Therefore, in this study, we utilize VnGP as the reference for the gridded observation data sets.

#### *2.1.2. APHRODITE*

The APHRODITE data set is a product of the Research Institute for Humanity and Nature (RIHN) and the Meteorological Research Institute of Japan Meteorological Agency (MRI/JMA). The APHRODITE project developed state-of-the-art daily precipitation data sets at high-resolution grids (0.25 and 0.5°) for Monsoon Asia. This study uses the 0.25° data set of the Monsoon Asia region for the period 1951–2007. The data sets were created primarily with data obtained from rain gauge observation network. The daily precipitation values from rain gauges were interpolated using the Spheremap technique (Wilmott *et al.*, 1985) and the first six components of the fast Fourier transforms were taken to obtain daily data for all land areas in the Monsoon Asia region (Yatagai *et al.*, 2012). The number of rain gauges used to interpolate from the station to the gridded data set for APH in shown in Figure 1(b). As seen in this figure, this product has higher station density per grid cell compared to the other data sets. This data set is referred to as 'APH' in this article, for brevity.

#### *2.1.3. Climatic research unit*

The climatic research unit (CRU) time series (TS) latest version 3.24 data set (Harris *et al.*, 2014) was used in this study. These data sets comprise of monthly grids

 

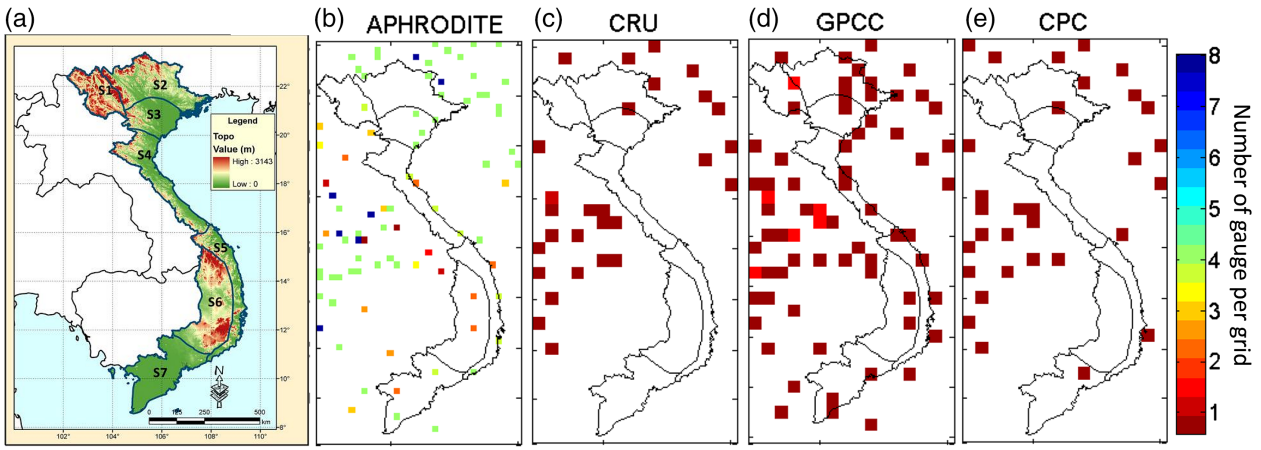


Figure 1. (a) Seven climate sub-regions of Vietnam (S1–S7) overlaid on Vietnam topography by SRTM (90 m); number of rain gauge per grid cell for each data set (except UDEL) used in the study, the number next to each data set is the total number of rainfall stations located inside the country: (b) APHRODITE '24', (c) CRU '1', (d) GPCC '27' and (e) CPC '4'. [Colour figure can be viewed at wileyonlinelibrary.com].

Table 2. Classification of SPI for drought and wet category.

| SPI values | Category | Time in category (%) |
|---|---|---|
| ≥2.00 | Extreme wet | 2.3 |
| 1.5–1.99 | Severe wet | 4.4 |
| 1–1.49 | Moderate wet | 9.2 |
| −1 to 1 | Near normal | 68 |
| −1 to −1.49 | Moderate drought | 9.2 |
| −1.5 to −1.99 | Severe drought | 4.4 |
| ≤−2 | Extreme drought | 2.3 |

Table 3. Climate sub-region of Vietnam.

| Sub-region climate | Name |
|---|---|
| Northwest | S1 |
| NE | S2 |
| Red River Delta | S3 |
| North Central | S4 |
| South Central | S5 |
| Central Highland | S6 |
| South | S7 |

of observed climate for the period 1901–2015 at a 0.5° horizontal spatial resolution. CRU obtains station data from different sources: Global Historical Climatology Network (GHCN-v2) and data internationally exchanged over the World Meteorological Organization (WMO) official international climate monitoring (CLIMAT) network (Jones and Moberg, 2003). The angular distance weighted (ADW) technique was applied to interpolate precipitation grid cell from eight nearest stations (Wilmott *et al.*, 1985). This data set is one of the most extensively used data sets by the climate modelling community. The precipitation used in this study comprises data obtained from many land locations around the globe. The number of stations for precipitation is large and it changed over time (i.e. nearly 13 000 stations in 2000). However, there is only one station in Vietnam that was used in interpolating the CRU data set, averaging over the study period (Figure 1(c)). Further information on these data sets is available at http://www.cru.uea.ac.uk/cru/data and is documented in earlier publications by New *et al.* (1990, 2000) and Mitchell and Jones (2005).

### 2.1.4. *Global Precipitation Climate Center*

The Global Precipitation Climate Center (GPCC)'s full data reanalysis (V.7) is a gauge-based gridded monthly precipitation data set for the global land surface, available at a spatial resolution of 0.5°. GPCC is the official precipitation data of the WMO. The v7 data set covers the period from 1901 to 2013 and is based on both non-real-time and real-time quality controlled data from 67 200 stations world-wide that feature record durations of 10 years or longer (Becker *et al.*, 2013). The gridded data are spatially interpolated by modified spherical adaptation (Wilmott *et al.*, 1985). Several quality controls, data harmonization and inter-comparison of different sources have been applied to all rain gauges before interpolation (Becker *et al.*, 2013). Over Vietnam, GPCC used a large number of rain gauge station (Figure 1(d)) compared to other data sets. It even has a higher number of stations compared to the APH with a denser network along the coast line; however, the density of station is about one station per grid cell over the country.

### 2.1.5. *University of Delaware*

This monthly gridded, land only, global high-resolution precipitation station data (0.5°) was developed at the University of Delaware (UDEL) from a large number of stations from the GHCN-v2, Global Summary of the Day (GSOD), National Climatic Data Center (NCDC) and more extensively, from the archive of Legates and Willmott (1990). Traditional interpolation techniques that utilized the distance weighting approach of Shepard (1968) and Wilmott *et al.* (1985) were applied to construct this gridded data. The version v4.01 spans from 1901 to 2014 and can be downloaded from the web site at http://www.esrl.noaa.gov/psd/.

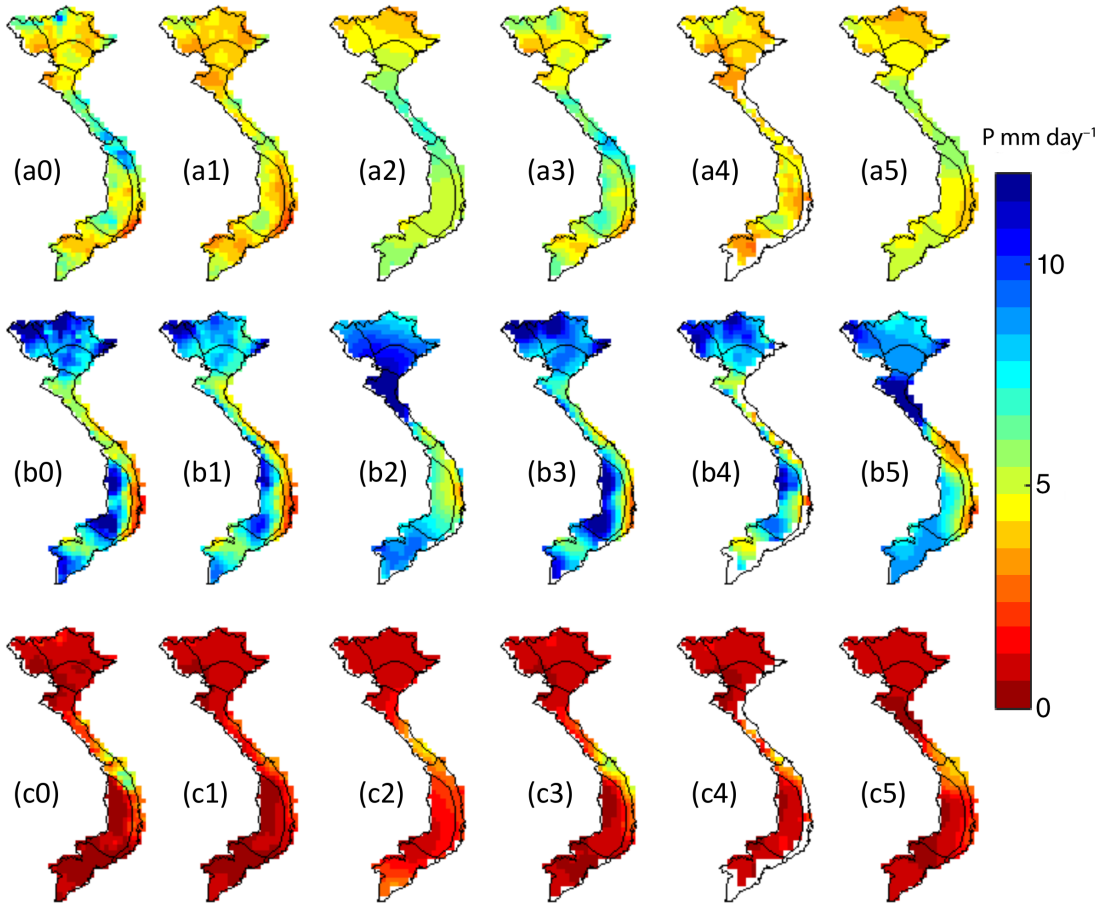


Figure 2. Mean precipitation for (a) annual, (b) SW monsoon (JJA) and (c) NE monsoon (DJF). Notation indices: (0) VnGP, (1) APH, (2) CRU, (3) GPCC, (4) UDEL, (5) CPC. [Colour figure can be viewed at wileyonlinelibrary.com].

#### *2.1.6. Climate Prediction Center*

This Climate Prediction Center (CPC)'s global data product was developed by the interpolation of National Oceanic and Atmospheric Administration's PRECipitation REConstruction over Land (PREC/L) and by the reconstruction of historical observations over the ocean. This product was derived from gauge observations from over 17 000 stations collected under the GHCN and the Climate Anomaly Monitoring System (CAMS) data sets. The monthly grid cell is constructed by Gandin optimal interpolation approach (Gandin, 1965) for precipitation anomaly and Shepard (1968) for the long-term mean. This global rainfall data set was initially developed at a 2.5° resolution and now is available at a 0.5° resolution, which is used in this study for the period 1961–2007. The details about these data sets are available in the study by Chen *et al.* (2002). Similar to CRU, CPC does not have many rain gauges over Vietnam (Figure 1(e)), especially in the coastal regions.

### 2.2. Standardized Precipitation Index

The SPI was first introduced by McKee *et al.* (1993) and it is calculated using following steps (Guttman, 1999): (1) identify a probability density function that best fit the long-term TS of rainfall observations; (2) construct a set of moving windows of the rainfall observation series depending on the time scale of interest. Here we constructed moving windows of total precipitation corresponding to 3, 6 and 12 months to derive SPI 3, SPI 6 and SPI 12, respectively; (3) apply the selected probability density function to the TS (from step 2) to construct the cumulative probability distribution and (4) apply the inverse normal (Gaussian) function (with mean zero and variance one) to the cumulative probability distribution function to construct the SPI TS. Based on the Kolmogorov–Smirnov (K–S) and chi-square test statistics, we found that the monthly rainfall series followed a gamma distribution. The detailed SPI calculation procedure can be found in the studies by McKee *et al.* (1993) and Mishra and Desai (2005a, 2005b). The SPI values that define the categories of drought and wetness are tabulated in Table 2.

SPI is flexible as it only requires precipitation as input. In the present study, drought and wetness were classified using SPI 3, SPI 6 and SPI 12 TS. In general, the mean drought duration is higher for SPI 12, followed by SPI 6 and SPI 3 (Mishra and Desai, 2005b). However, the standardization of the SPI ensures that the frequencies of extreme events at any location and at any time scale are consistent. A threshold of 1.5 is selected to identify severe drought/wetness and it is used to calculate the drought/wetness characteristics based on of SPI.

 

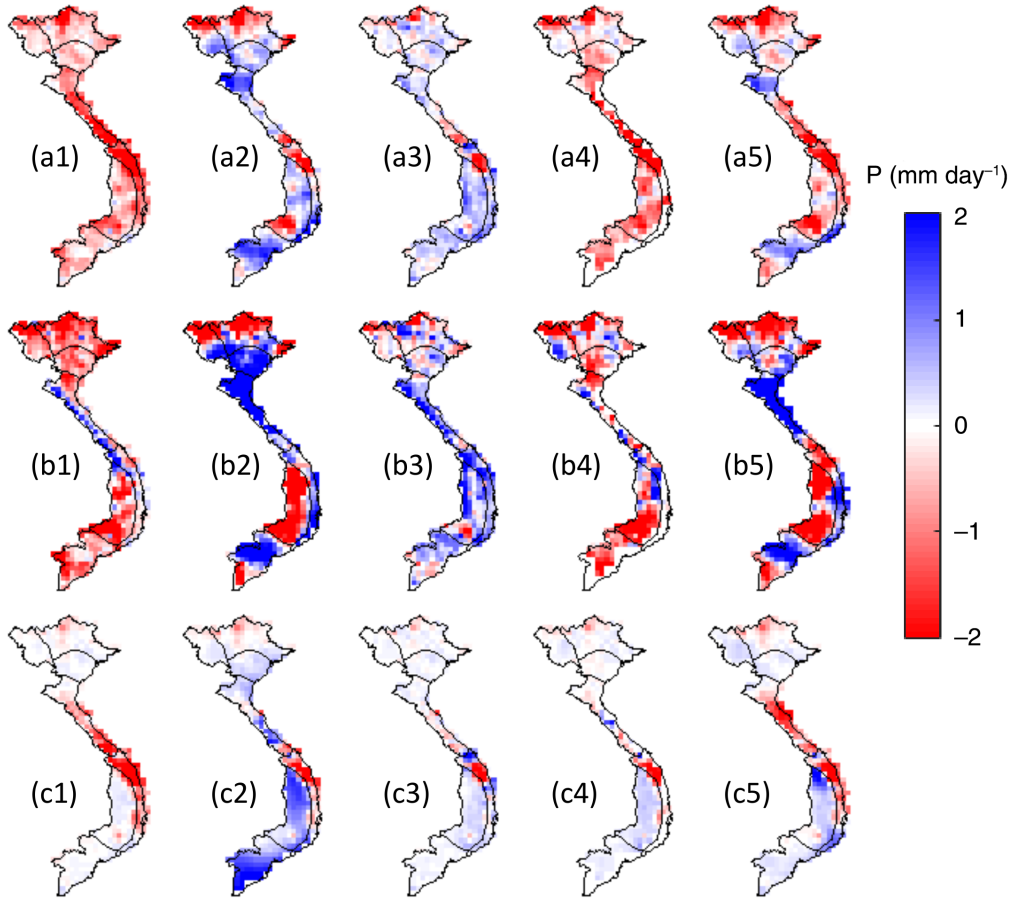


Figure 3. Biases in precipitation: VnGP *versus* gridded data for: (a) annual, (b) SW monsoon (JJA), (c) NE monsoon (DJF). Notation indices: (1) APH, (2) CRU, (3) GPCC, (4) UDEL and (5) CPC. [Colour figure can be viewed at wileyonlinelibrary.com].

## 2.3. Trend analysis

### *2.3.1. Mann–Kendall test*

Mann–Kendall (MK) test is widely used for trend analysis in hydrology and climate related studies; e.g. application of MK test to precipitation (Partal and Kahya, 2006; Mishra *et al.*, 2009; Tabari and Talaee, 2011b; Gocic and Trajovic, 2013), temperature (Tabari and Talaee, 2011a; Gocic and Trajovic, 2013), flood and low flows (Douglas *et al.*, 2000; Mishra *et al.*, 2010) and streamflow (Birsan *et al.*, 2005; Novotny and Stefan, 2007).

As MK test is a nonparametric test, it does not require the data to be distributed normally. However, the SPI values are calculated using a moving window concept; hence, it has a serial correlation effect and it may not be directly used in MK test. Therefore, to overcome this limitation, we used modified MK (MMK) test suggested by Hamed and Rao (1998). The detailed methodology to generate MMK trend test can be found in the study by Vu *et al.* (2015, 2016). The positive values of MK $Z$ indicate increasing trends (upwards trend) while negative $Z$ indicate decreasing trends (downwards trend). When testing either increasing or decreasing monotonic trends at the $\alpha$ significance level, the null hypothesis was rejected for an absolute value of $Z$ greater than that is obtained from the standard normal cumulative distribution tables (Tabari and Talaee, 2011b; Gocic and Trajovic, 2013). In this article, at a statistical significance level of $\alpha = 0.05$ the trend detected by the $Z$ value is significant at $|Z| \geq 1.96$.

### *2.3.2. Sen's slope estimator*

If a linear trend is present in a TS, then the true slope (change per unit time) can be estimated by using a simple nonparametric procedure developed by Sen (1968). The slope estimates of $N$ pairs of data are first computed by

$$Q_i = \frac{x_j - x_k}{j - k} \quad \text{for } i = 1, \ldots, N \tag{1}$$

where $x_j$ and $x_k$ are data values at time $j$ and $k$ ($j > k$). The median of these $N$ values of $Q_i$ is Sen's estimator of slope (Partal and Kahya, 2006). Sen's slope has been used in many other studies (Tabari and Talaee, 2011a, 2011b; Paulo *et al.*, 2012; Vu *et al.*, 2015; Vu and Mishra, 2016) to quantify the true slopes of trend studied variables. In this study, Sen's slope estimator was applied to find the slope for SPI 6 over the study region. It was computed and analysed spatially.

## 2.4. Data analysis

All the gridded data sets were re-gridded (using bilinear interpolation) to a common 0.25° resolution to match with

 

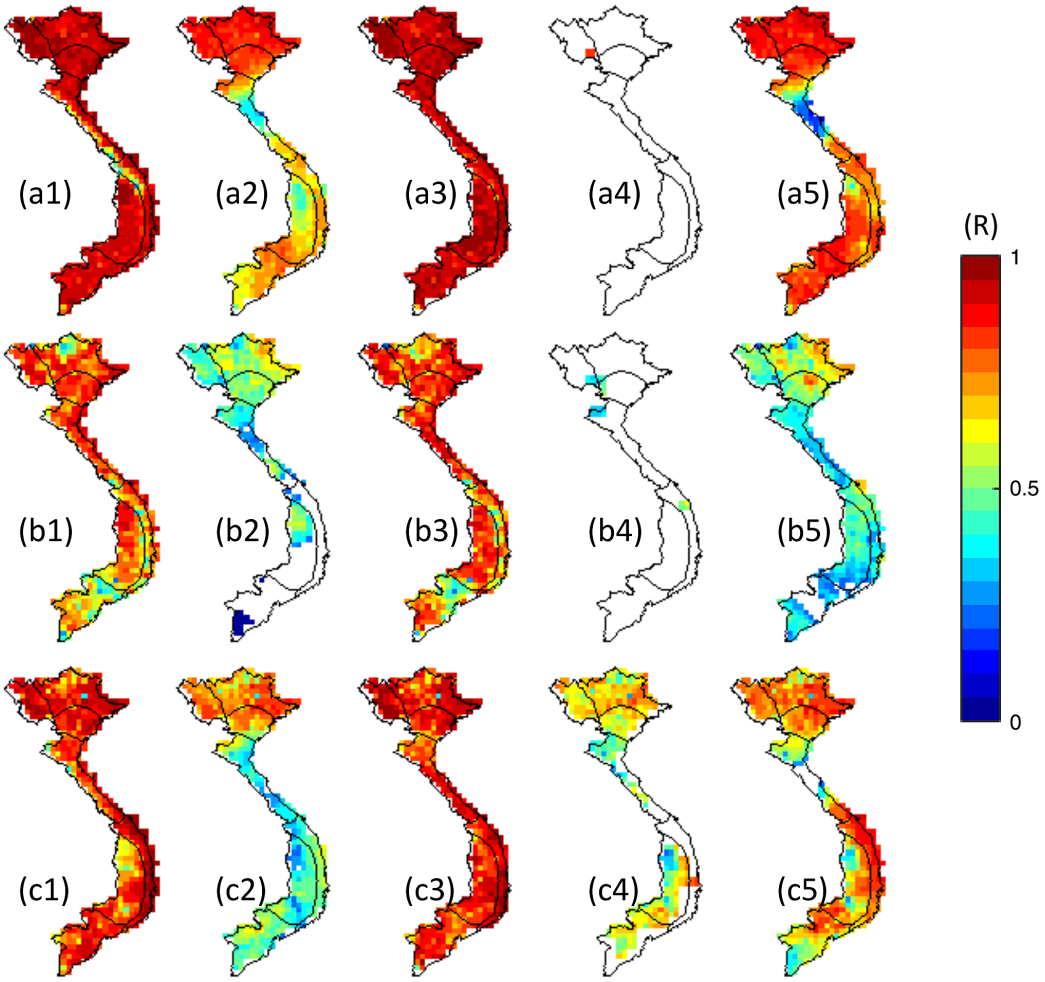


Figure 4. Temporal Pearson correlations of the gridded data *versus* VnGP: (a) annual, (b) SW monsoon (JJA), (c) NE monsoon (DJF). Notation indices: (1) APH, (2) CRU, (3) GPCC, (4) UDEL and (5) CPC. Only correlations with $p$ values $\leq 0.05$ are displayed. [Colour figure can be viewed at wileyonlinelibrary.com].

the reference observation data sets. A common period of 28 years (1980–2007) available for all data sets was chosen for the analysis. This time frame covers some of the severe drought and wet events that are associated with strong El Nino Southern Oscillation (ENSO) years (strong El Nino in 1982, 1991 and 1997; strong La Nina in 1988 and 1999) (Vu *et al.*, 2013). This is significant as Vietnam is highly influenced by the ENSO events. The comparison between these data sets was made based on the total precipitation and SPI using the statistical approaches [mean, bias, standard deviation (SD), root-mean-square difference (RMSD) and Pearson correlation (R)] at different spatio-temporal scale. The dry month (November 1982) due to strong El Nino and wet month (December 1999) due to strong La Nina are also displayed on a spatial map. As Vietnam is located in a tropical monsoon region and also bears highly complex topography, it is divided into seven climate sub-regions (Phan *et al.*, 2009). The demarcations of these seven sub-regions (S1–S7) are displayed in Figure 1(a), overlaid on the Shuttle Radar Topography Mission (SRTM), Digital Elevation Model (DEM) at 90 m spatial resolution. An overview of these climate sub-regions is provided in Table 3. Because of this classification into seven climate sub-regions, their areal averages are computed and compared based on the severe to extreme drought/wetness characteristics, such as percentage and severity of wet/dry events, mean inter-arrival time and percent of grids undergoing drought/wetness in terms of spatio-temporal scale between these five gridded precipitation data sets. Finally, trend analyses were computed to quantify the variability of SPI 6 indices over annual and seasonal time scale.

## 3. Results and discussions

### 3.1. Evaluation of spatial distributions of precipitation

The gridded data sets are compared with observed data using mean precipitation climatology for the study period 1980–2007 using three different time scales: annual, northeast (NE) monsoon [December–January–February (DJF)] and southwest (SW) monsoon [June–July–August (JJA)]. The VnGP data set (Figures 2(a0)–(c0)) apparently shows the distributions of precipitation over Vietnam due to complex topography as shown earlier in Figure 1(a). It was observed that regions (S4 and S5) have distinct

 

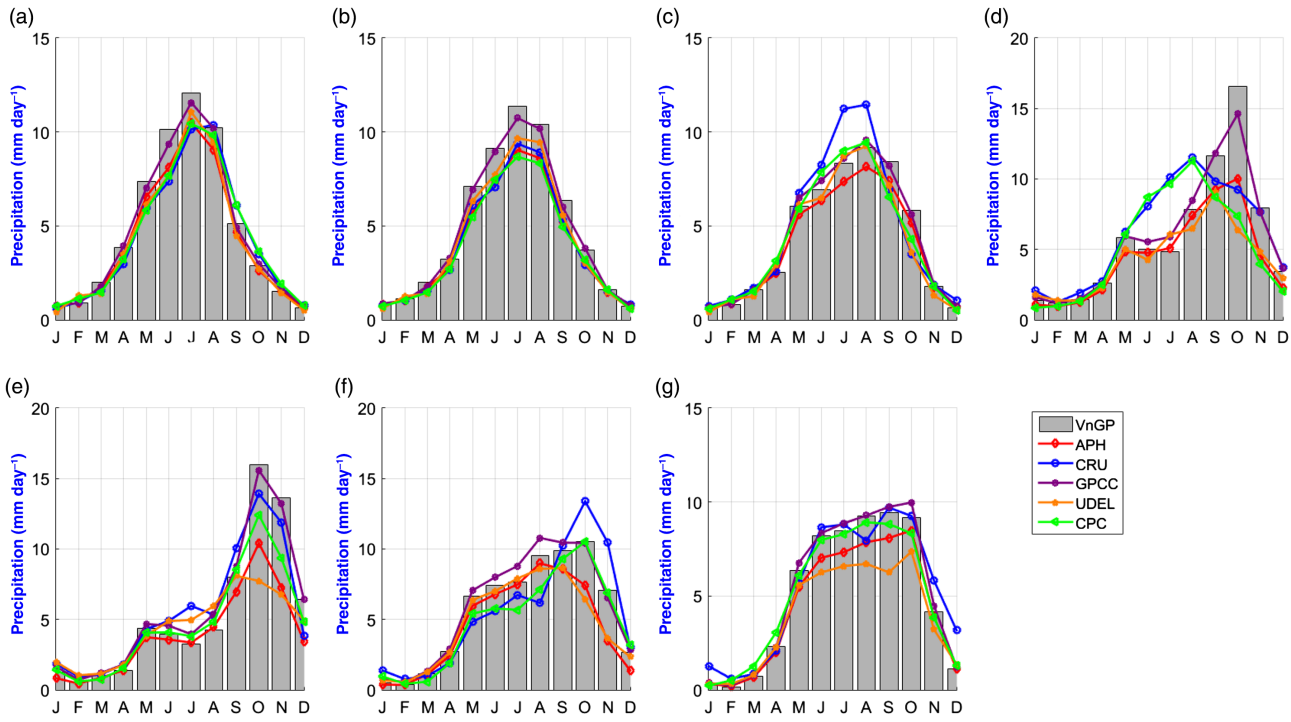


Figure 5. Annual cycle rainfall for all sub-regions over Vietnam; sub-region: (a) S1, (b) S2, (c) S3, (d) S4, (e) S5, (f) S6 and (g) S7. [Colour figure can be viewed at wileyonlinelibrary.com].

precipitation patterns compared to other sub-regions, especially during monsoon seasons (Figures 2(b0) and (c0)). They are drier during the SW monsoon (Figure 2(b0)) and wetter during the NE monsoon (Figure 2(c0)).

On an annual scale (Figure 2(a)), it was observed that the gridded data sets show discrepancies for different spatial domains. When compared to VnGP, the APH and UDEL data sets (Figures 2(a1) and (a4)) underestimate the precipitation patterns over regions (S4 and S5) compared to their counterparts CRU, GPCC and CPC in terms of spatial patterns. However, nearly all gridded data sets fail to capture the highest rainfall (seen as a blue spot in Figure 2(a0)) near the Fansipan mountain peak (3143 m) located in region S2. This may be because all gridded data sets were derived from a coarser resolution of station data compared to VnGP. On the other hand, GPCC is able to marginally capture this highest rainfall (Figure 2(a3)) and it is able to capture the spatial pattern of observed data (VnGP). There are some missing data points over the coastal areas in sub-regions (S4, S5 and S7) in the UDEL data, this may be due to its inter/extrapolation technique from sparse station data (Figure 2(a4)).

The SW monsoon seasonal rainfall was captured well by the gridded data sets as seen in Figure 2(b). A dry central coastline in S4 and S5 is observed for both the station and the gridded data sets. This feature occurs because the Annamite mountain range obstructs the SW monsoon wind coming from Laos and it causes an effect called 'foehn' over sub-regions S4 and S5 (Ho *et al.*, 2011). As a result, the monsoon rainfall is experienced on the west side of the mountains and a dry and hot climate over the S4 and S5 regions. Such a pattern was clearly observed by all gridded data, especially APH. The NE monsoon rainfall is low as it coincides with the dry season and its spatial distribution was captured well by the gridded data as seen in Figure 2(c). The heavy rainfall observed in VnGP (Figure 2(c0)) and gridded data at the border regions (S4 and S5) is the result of the Annamite range that obstructs the NE monsoon coming from China. This pattern is clearly pronounced in the all gridded data sets but relatively less in APH.

The bias between the VnGP and the gridded data sets were observed (Figure 3) based on the annual and seasonal time scales. At the annual time scale (Figure 3(a)): (1) APH and UDEL overestimated the rainfall, (2) CRU and GPCC underestimated the rainfall over most part of the study domain, whereas CPC shows positive (negative) biases across the country and (3) specifically most of the gridded data sets underestimated the high rainfall pattern over the border region between S4 and S5, which could be attributed to the complex topography of the region. All gridded data sets were able to capture the dry season 'DJF' (Figure 3(c)) over the sub-regions S1, S2, S3, S6 and S7 except CRU that overestimated in S6 and S7 regions.

Figure 4 displays the Pearson correlation coefficients computed for each pixel between the gridded data and VnGP on a monthly scale and only correlation values with $p$ values $<0.05$ are displayed. It can be seen that APH and GPCC are the only two gridded data sets having a 'near perfect' correlation with VnGP at the annual and the dry season (Figures 4(a1), (a3), (c1) and (c3)). The UDEL, however, has insignificant correlations for annual and SW monsoon (Figures 4(a4) and (b4)), while CRU has insignificant correlation for S5, S6 and S7

 

sub-regions during SW monsoon season (Figure 4(b2)). CPC has higher correlation compared to CRU and UDEL but it is lower than APH and GPCC for annual and the two seasons.

### 3.2. Evaluation of temporal precipitation pattern

The temporal distribution of precipitation was compared between VnGP and five different gridded sets based on the areal average of the grid cells for each sub-region. The annual cycles of precipitation pattern for the seven sub-regions are displayed in Figure 5. It can be observed that the temporal distribution of precipitation differs for selected sub-regions. The observed data set (i.e. VnGP) shows similar annual precipitation cycle for regions S1 and S2 (Figures 5(a) and (b)) with the peak (maximum) occurring in July, while the peak is shifted to August for region S3 (Figure 5(c)). The southern part of study area including regions S4 and S5 exhibits a peak rainfall during the inter-monsoon season Sep–Oct–Nov (SON) (Figures 5(d) and (e)). Regions S6 and S7 clearly display distinct wet and dry seasons (Figures 5(f) and (g)). Among all gridded data set, GPCC shows a good agreement with VnGP in terms of the peak rainfall and the sub-region annual cycles. Although APH follows the annual precipitation patterns at all sub-regions but marginally underestimates the peak rainfall. In particular, UDEL underestimates precipitation over sub-regions S5 and S6 during the months from September through to December and most of the months in S7. CRU overestimates for few months for sub-regions S3, S4 and S6. CPC shows good agreement in the annual cycles over all sub-regions except in S4.

The Taylor diagram analysis was used to investigate uncertainties in the different data sets (against VnGP) in terms of the correlation coefficient, SD and the RMSD (Figure 6). The Taylor diagram suggests that GPCC is the best data set in temporal scale due to its highest correlation (>0.97), smallest RMSD (<35 mm/month) and a lower SD range compared to VnGP. APH performs well as the next best data set with comparatively lower correlation for four

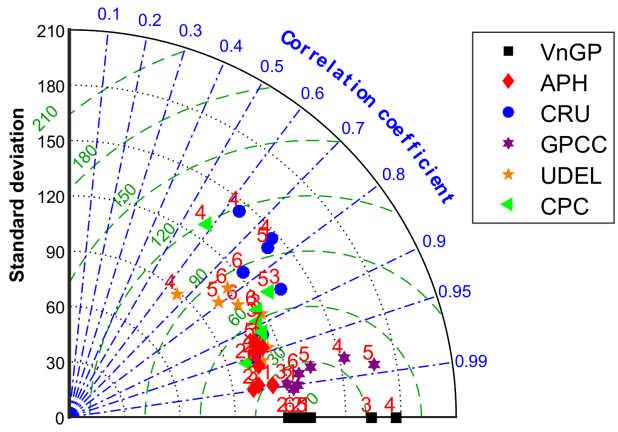


Figure 6. Taylor diagram: monthly total precipitation between VnGP and the gridded data sets. The unit is mm/month. Different markers indicate different data sets. The sub-regions are displayed as corresponding number. [Colour figure can be viewed at wileyonlinelibrary.com].

sub-regions and higher RMSD compared to GPCC. APH has consistently lower SD against VnGP, especially for sub-regions S4 and S5. CRU, CPC and UDEL show lower correlations and larger RMSD. However, in terms of the SD, CRU performs better than CPC, UDEL and APH.

### 3.3. Evaluation of drought and wetness during El Nino and La Nina

All the gridded data sets are evaluated for drought and wetness events using SPI during the strong El Nino and La Nina years. The ENSO has been known to be a teleconnection phenomenon and it has a potential impact on Vietnam precipitation. During 1980–2007, there were three strong El Nino phases (1982, 1991 and 1997) and two La Nina phases (1988 and 1999) (Phan *et al.*, 2009). In this study, we consider one strong El Nino phase in November 1982 and one strong La Nina phase in December 1999 for analysis. The SPI 6 was selected for wet and dry analysis for two selected periods (Figures 7(a) and (b)). Although SPI 12 and SPI 3 generated similar results, the discussion was focused only on SPI 6.

Based on VnGP, El Nino brings more drought ($SPI < -1.5$ indicates severe to extreme drought) to sub-regions S4–S7 (Figure 7(a0)). Few gridded data sets (APH and GPCC) are able to reproduce the spatial drought pattern compared to VnGP. However, CPC is partially able to capture this spatial pattern, but it depicts extreme drought over the Mekong delta in sub-region S7. Overall, CRU and UDEL did not perform well in capturing the SPI patterns for this drought event. The strong La Nina event in December 1999 (Figure 7(b)) depicts the opposite pattern compared to the strong El Nino event, represented by extreme wetness over sub-regions S4 and S5. This pattern can be seen in nearly all the gridded data sets except UDEL, possibly due to some missing data over the coastal areas.

### 3.4. Evaluation of sub-regional SPI

The sub-regional average SPI was calculated for gridded data sets and compared with VnGP data using goodness-of-fit tests (SD, R and RMSD) and displayed using a Taylor diagram (Figure 8). For each of the sub-region, the SD of all data sets is equal to 1 because SPI values are standardized. Therefore, we only compared correlation 'R' and RMSD using SPI 6. Among all seven sub-regions, GPCC agrees well based on higher R and lower RMSD values. The second best data are APH especially for sub-regions S1–S5. The other three data sets showed mixed performance, with CRU performing well over sub-regions S1 and S2, whereas CPC for regions S3 and S7.

### 3.5. Evaluation of spatio-temporal drought and wetness

Spatio-temporal drought information is useful for water resources planning and management (Mishra and Singh, 2010). SPI 6 was used to quantify severe to extreme drought events ($SPI < -1.5$) as well as wet spells ($SPI > 1.5$). The spatio-temporal pattern was compared

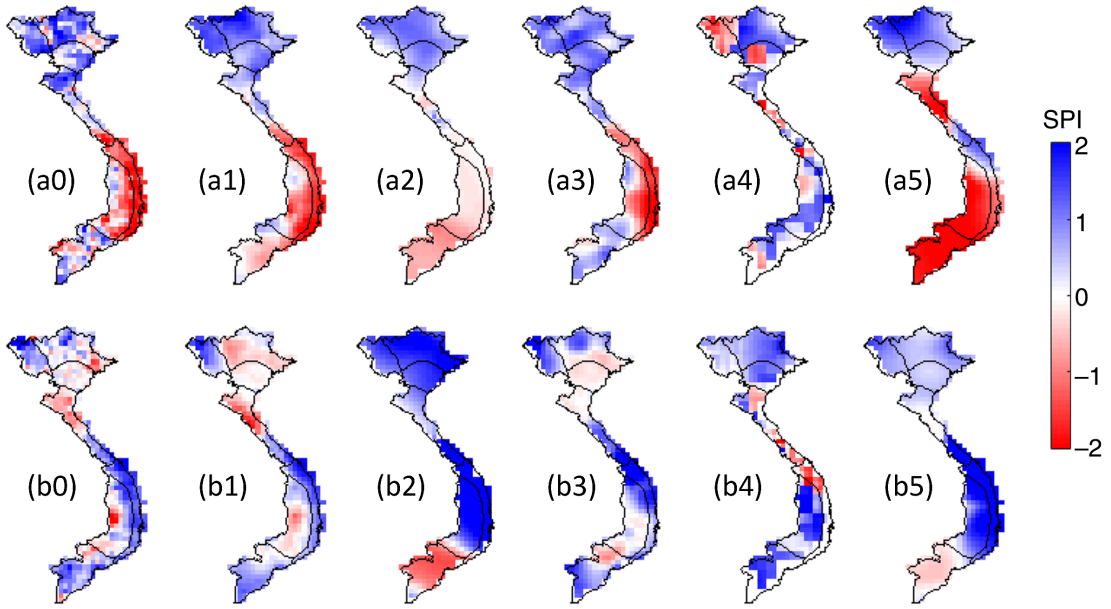


Figure 7. Spatial distributions of SPI for 6-month accumulations during (a) November 1982, strong El Nino year and (b) December 1999, strong La Nina year. Notation indices: (0) VnGP, (1) APH, (2) CRU, (3) GPCC, (4) UDEL, (5) CPC. [Colour figure can be viewed at wileyonlinelibrary.com].

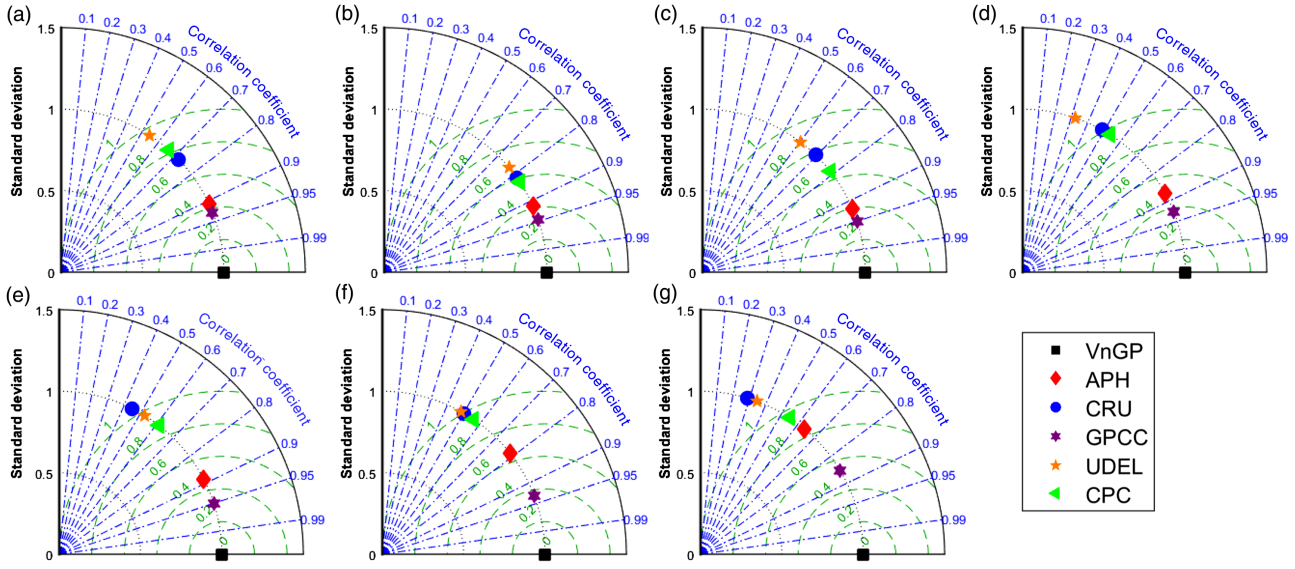


Figure 8. Taylor diagram: SPI 6 between VnGP and gridded data sets: (a) S1, (b) S2, (c) S3, (d) S4, (e) S5, (f) S6 and (g) S7. [Colour figure can be viewed at wileyonlinelibrary.com].

between gridded and observed data sets based on three indicators: (1) Percentage of wet/dry months: This is computed by summing the total number of wet/dry months for the study period, then divided by total number of months, subsequently multiplied by 100 to obtain the percentage value. (2) Severity of wet/dry month: This characteristic is similar to the total wet/dry months, but instead of counting number of months, it adds the corresponding SPI value for the wet/dry months. (3) Mean inter-arrival time: The interval time (in month) between two consecutive dry/wet spells are computed for all the months in the study period. Subsequently, the TS of the inter-arrival time are calculated for each dry/wet event. The average of the TS is the so called mean inter-arrival time.

The drought and wetness characteristics are displayed in Figures 9 and 10, respectively. The percentage of dry and wet events for SPI 6 found to be 5–7% (Figures 9(a) and 10(a)). The spatial-temporal characteristics of drought and wetness events are evaluated using SPI 6 based on observed data and gridded data sets for all sub-regions (Table 4). Overall gridded data sets agree well with observed data set (i.e. VnGP) for distributions of drought characteristics, except UDEL for sub-regions S1–S5. Based on both wet/dry characteristics of percentage and severity, GPCC agrees well in sub-regions S1 and S2, whereas APH agrees well in S3, S5 and S6 and CRU in S4 and S6 (Table 4). The mean inter-arrival time exhibits a clear difference between the gridded data and

 

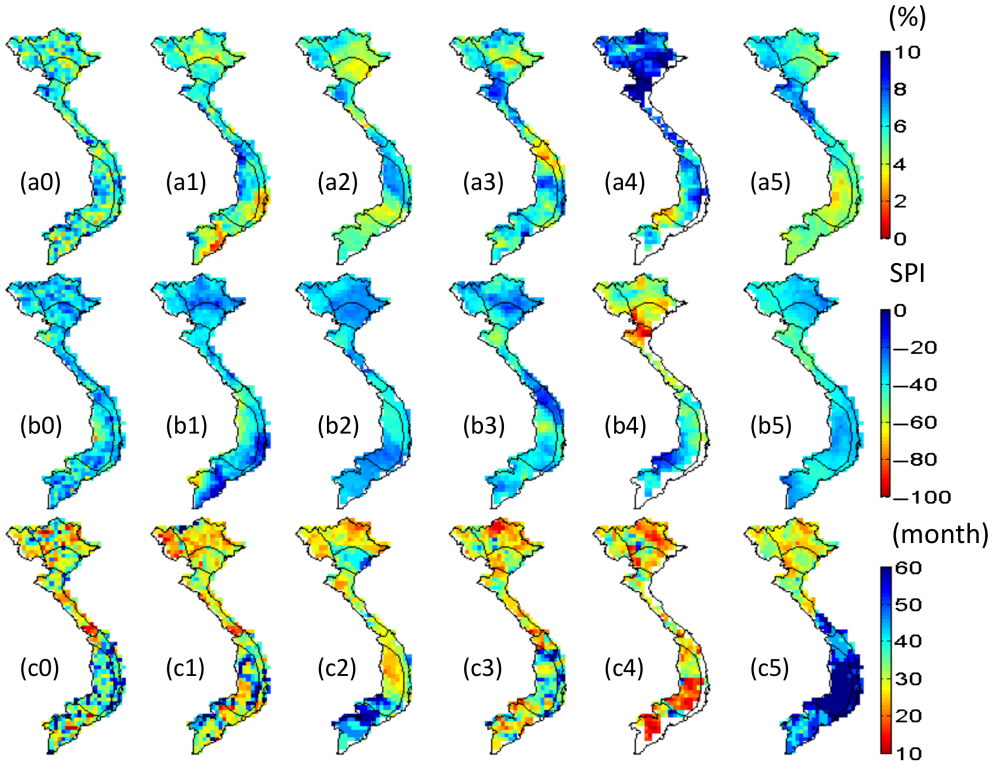


Figure 9. Drought characteristics from SPI 6: (a) percentage of drought (%) (percentage of total number of dry months over all months in the study period); (b) drought severity (unit less) (total SPI values for the dry months); (c) mean inter-arrival time (month) (average time intervals between two consecutive dry spells). Notation indices: (0) VnGP, (1) APH, (2) CRU, (3) GPCC, (4) UDEL, (5) CPC. [Colour figure can be viewed at wileyonlinelibrary.com].

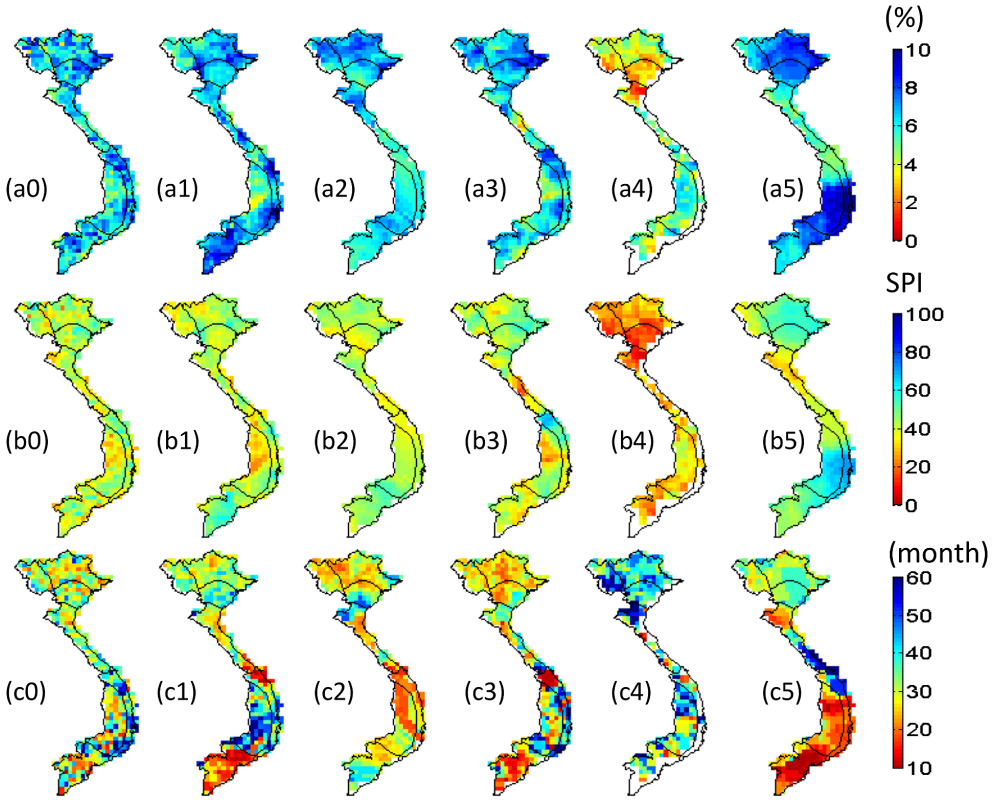


Figure 10. Wetness characteristics from SPI 6: (a) percentage of wetness (%) (percentage of total number of wet months over all months in the study period); (b) wetness severity (unit less) (total SPI values for the wet months); (c) mean inter-arrival time (month) (average time intervals between two consecutive wet spells). Notation indices: (0) VnGP, (1) APH, (2) CRU, (3) GPCC, (4) UDEL, (5) CPC. [Colour figure can be viewed at wileyonlinelibrary.com].

 

Table 4. Drought and wetness characteristics (percentage and severity) between gridded observation data and station data for all sub-regions, based on SPI 6.

| Data | VnGP | APH | CRU | GPCC | UDEL | CPC |
|---|---|---|---|---|---|---|
| *S1* | | | | | | |
| Drought percentage | 5.2 | 6.8 | 7.1 | **5.9** | 7.4 | 7.4 |
| Drought severity | −31.5 | −39.9 | −41.5 | **−32.9** | −46.9 | −46.2 |
| Wetness percentage | 8.6 | 7.1 | 7.1 | **7.7** | 6.2 | 7.1 |
| Wetness severity | 50.9 | 43.4 | 41.9 | **48.0** | 34.9 | 44.0 |
| *S2* | | | | | | |
| Drought percentage | 6.2 | **5.6** | **5.6** | **6.8** | 7.4 | **5.9** |
| Drought severity | −35.3 | −31.0 | **−32.8** | **−39.1** | −47.5 | **−34.7** |
| Wetness percentage | 7.1 | **7.1** | 8.3 | **7.4** | 5.2 | 9.0 |
| Wetness severity | 44.7 | **45.4** | 51.5 | **47.4** | 34.2 | 58.8 |
| *S3* | | | | | | |
| Drought percentage | 7.7 | 6.2 | 4.3 | 4.9 | **8.3** | 5.6 |
| Drought severity | −45.0 | **−37.0** | −28.8 | −29.1 | −58.3 | −36.3 |
| Wetness percentage | 6.2 | **6.5** | 7.4 | 7.1 | 3.1 | 8.0 |
| Wetness severity | 40.6 | **38.6** | 45.8 | 46.0 | 20.7 | 53.7 |
| *S4* | | | | | | |
| Drought percentage | 5.9 | 6.8 | **6.2** | 7.1 | 10.5 | 7.1 |
| Drought severity | −36.1 | −41.8 | **−37.9** | −41.6 | −70.3 | −46.5 |
| Wetness percentage | 7.1 | 8.3 | 8.6 | **7.4** | 2.2 | 6.2 |
| Wetness severity | 46.0 | 54.0 | **47.8** | **48.1** | 11.7 | 38.4 |
| *S5* | | | | | | |
| Drought percentage | 5.9 | **6.2** | **6.2** | 4.3 | 9.9 | **5.6** |
| Drought severity | −35.9 | **−37.9** | **−37.9** | −25.7 | −64.1 | **−36.3** |
| Wetness percentage | 9.0 | **9.6** | 5.9 | 7.4 | 4.3 | **9.6** |
| Wetness severity | 54.6 | **55.0** | 40.4 | **54.3** | 27.3 | 64.0 |
| *S6* | | | | | | |
| Drought percentage | 7.4 | 6.5 | **7.1** | 6.2 | **7.1** | 4.3 |
| Drought severity | −45.6 | **−41.6** | **−41.6** | −36.5 | −40.0 | −31.7 |
| Wetness percentage | 7.1 | **6.8** | **6.5** | 8.0 | 8.3 | 8.6 |
| Wetness severity | 42.7 | **40.0** | **44.0** | 55.8 | 48.1 | 58.4 |
| *S7* | | | | | | |
| Drought percentage | 6.8 | 4.9 | 5.2 | **6.5** | 5.2 | 4.0 |
| Drought severity | −43.4 | −31.3 | −31.9 | **−36.8** | −29.6 | −29.1 |
| Wetness percentage | 5.6 | 8.6 | 7.1 | 7.4 | **5.6** | 6.8 |
| Wetness severity | 36.5 | 57.3 | 50.2 | 47.2 | **31.6** | 47.9 |

The bold numbers represent less than 10% difference compared against VnGP.

VnGP (Figures 9(c) and 10(c)). APH and GPCC exhibit good match against VnGP for dry spell inter-arrival time (Figures 9(c1) and (c3)) but underestimates wet-spell for S7, although it is insignificant (Figures 10(c1) and (c3)). CRU is able to partially capture the spatial distribution of the mean inter-arrival time of wet/dry spells; however, UDEL and CPC are performed reasonably well only over certain sub-regions.

The spatial characteristics are further quantified by analysing the percentage of land affected by drought ($SPI < -1.5$) and wetness ($SPI > 1.5$) based on the number of grid points affected within the study domain for the study period 1981–2007 (Figures 11(a) and (b)). The correlation coefficients between gridded data and observed data (VnGP) based on a percentage of surface area affected by severe to extreme drought (wetness) is provided in Tables 5 and 6. Both APH and GPCC have significant correlations with VnGP for all sub-regions, but GPCC has a slightly higher correlation than APH. The poor performance of UDEL was observed in multiple sub-regions (S1, S4, S5 and S6), whereas poor performance was observed by CPC for sub-region S7. There are more significant (and higher) correlations for wetness category than drought for all gridded data sets over all sub-regions.

### 3.6. Evaluation of trend analysis for drought/wetness indices

Trend analyses were applied to compare the performance of all gridded data sets using SPI 6. First, the MMK trend tests were computed for all data sets to specify which regions have significant increasing/decreasing trend (at 5% significant level) over annual and seasonal time scale. Subsequently, Sen's slope was calculated for all the grids to quantify the change. Figure 12 displays the MMK trend tests for SPI 6. In this figure, blue colour denotes significant (at $Z = 0.05$) increasing trend ($Z \geq 1.96$) (towards wetter trend) and red colour indicates significant decreasing trend ($Z \leq -1.96$) (drier trend), the white colour are insignificant values ($-1.96 < Z < 1.96$). It is apparent that over the study period, significant increasing and decreasing trends of SPI 6 are observed for all data sets for annual and two seasons. The trend test reveals that for two monsoon (wet and dry) seasons, wetter trends are significant for SW monsoon season (or rainy seasons, Figure 12(b))

 

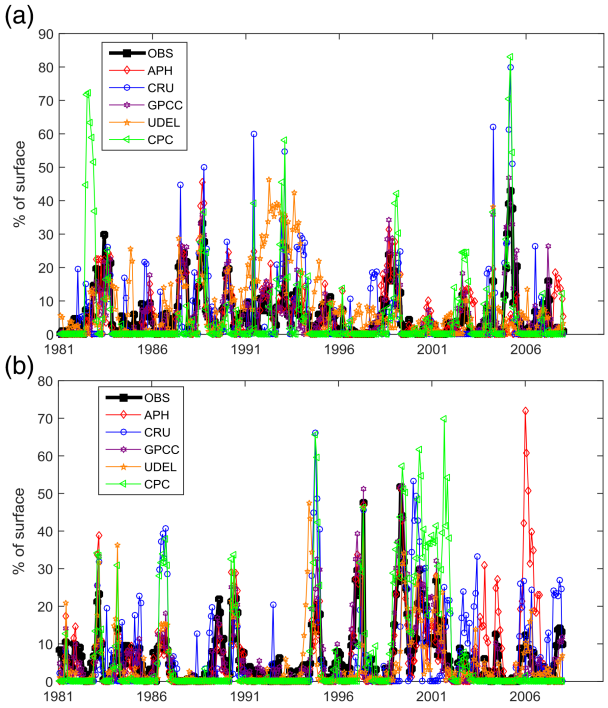


Figure 11. Percentage of surface area affected by (a) drought (b) wetness based on SPI 6 derived based on the observed and gridded data sets. Here SPI threshold of −1.5 (1.5) was used to determine severe to extreme drought (wetness) events. [Colour figure can be viewed at wileyonlinelibrary.com].

Table 5. Correlation coefficients between gridded data and VnGP for percentage of surface area affected by severe to extreme drought from 1980 to 2007.

| Region | APH | CRU | GPCC | UDEL | CPC |
|---|---|---|---|---|---|
| S1 | 0.81 | 0.28 | 0.72 | 0.10* | 0.27 |
| S2 | 0.84 | 0.59 | 0.86 | 0.43 | 0.60 |
| S3 | 0.88 | 0.60 | 0.89 | 0.38 | 0.65 |
| S4 | 0.78 | 0.57 | 0.87 | 0.04* | 0.47 |
| S5 | 0.82 | 0.17* | 0.88 | 0.14* | 0.31 |
| S6 | 0.43 | 0.44 | 0.91 | 0.03* | 0.41 |
| S7 | 0.55 | 0.03* | 0.76 | 0.23 | 0.14* |

*Insignificant correlations with $p$ values >0.01.

and it is replicated very well by all gridded data sets. Only GPCC and APH are able to capture the significant decreasing trend for Central Highland (sub-region S6) (Figures 12(b1) and (b3)). However, NE monsoon season (dry season) leads to the drier trend for northern Vietnam and wetter trend for central and southern Vietnam (Figure 12(c)). These trends are observed very well in all gridded data sets, but especially in APH, GPCC and UDEL (Figures 12(c1), (c3), and (c4)).

Subsequently, the quantification of changes in SPI 6 is illustrated (Figure 13) using Sen's slope analysis. It is noted that the magnitude of slopes computed for two seasons (Figures 13(b) and (c)) are nearly twice the values for annual scale (Figure 13(a)). The Sen's slopes values are comparatively small on the annual scale (Figure 13(a)) which implies that the temporal pattern of SPI 6 has little

Table 6. Similar to Table 5 but for wetness.

| Region | APH | CRU | GPCC | UDEL | CPC |
|---|---|---|---|---|---|
| S1 | 0.82 | 0.54 | 0.82 | 0.49 | 0.40 |
| S2 | 0.88 | 0.61 | 0.90 | 0.78 | 0.74 |
| S3 | 0.89 | 0.60 | 0.92 | 0.41 | 0.58 |
| S4 | 0.73 | 0.18 | 0.86 | 0.15 | 0.28 |
| S5 | 0.84 | 0.49 | 0.86 | 0.19 | 0.64 |
| S6 | 0.66 | 0.42 | 0.88 | 0.46 | 0.63 |
| S7 | 0.56 | 0.05* | 0.90 | 0.35 | 0.77 |

*Insignificant correlations with $p$ values >0.01.

fluctuation at this time scale. However, the increase in slope at the seasonal SPI 6 trends (Figures 13(b) and (c)) is likely to influence the frequency of drought and floods (Chou *et al.*, 2013). It is clearly seen that the Sen's slopes values for GPCC seem the best match with observation data, followed by APH and UDEL. Even though CPC is able to capture the variability of SPI 6 slopes spatially, its magnitude is comparatively poor among all gridded data sets.

## 4. Summary and conclusions

Five gridded precipitation data sets (APHRODITE, CRU, GPCC, UDEL and CPC) were compared against observed interpolated station data (VnGP) over Vietnam to test the ability of the gridded data in reproducing drought and wetness conditions. The period 1980–2007 was used for this comparison and the SPI was used for drought and wetness assessments for seven climatic sub-regions. The following conclusions are drawn from this study:

- Gridded data sets were able to capture the spatial distribution, mean biases as well as the temporal pattern of monthly precipitation when compared to observed data. Despite a coarser spatial and temporal resolution, GPCC seems to be the best among all the gridded data sets in reproducing the spatial patterns of precipitation at annual and seasonal scales. The second best gridded data set was APH. CPC, CRU and UDEL did not perform well in comparison with GPCC and APH.
- Based on Taylor diagram analysis for precipitation, GPCC outperforms all other gridded data sets for all metric indicators for seven sub-regions. GPCC was also able to capture the annual cycle with observed rainfall peak shifts over different sub-regions. APH has a marginal lower goodness-of-fit compared to GPCC, but it is significantly better than the other three precipitation data sets CRU, CPC, UDEL.
- Most of the gridded data (except UDEL) were able to capture the severe drought pattern during the strong El Nino event over the sub-regions S5 and S6. However, only GPCC and APH better resolve the wetness conditions induced by the strong La Nina event for sub-region S6.
- Several droughts and wetness characteristics such as the percentage of drought/wetness events, severity and mean inter-arrival time between dry/wet spells

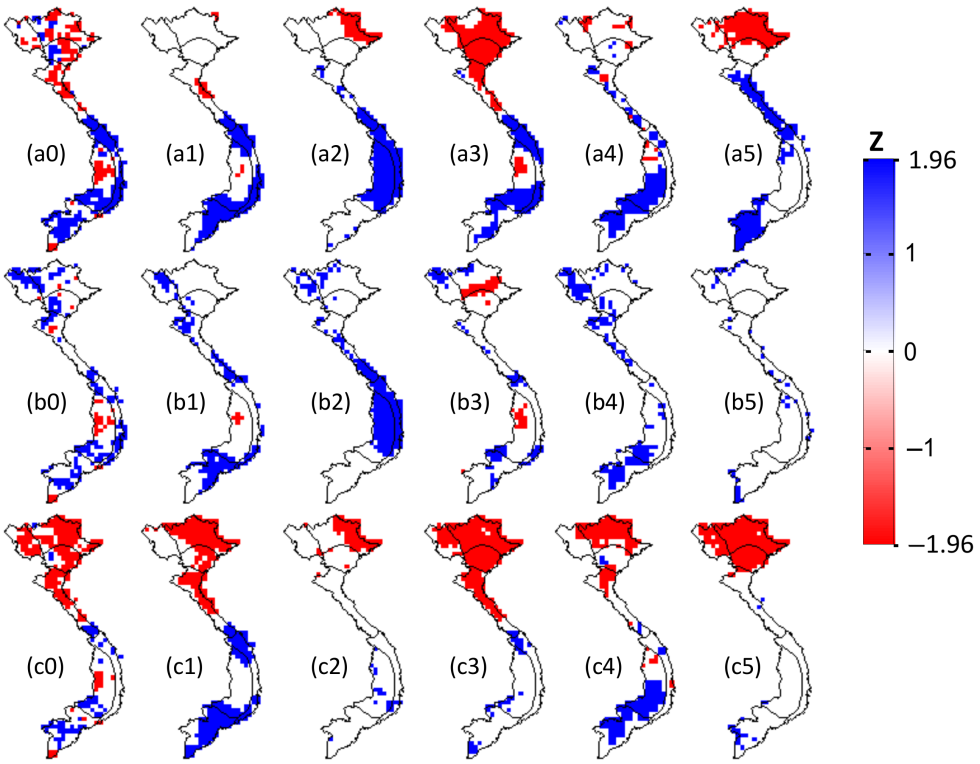


Figure 12. MMK $Z$ value for SPI 6 trend analysis, only significant levels 95% are displayed ($|Z| \geq 1.96$). Blue colour denotes significant increasing trend and red colour denotes significant decreasing trend, white colour are insignificant trends. (a) Annual, (b) SW monsoon (JJA), (c) NE monsoon (DJF). Notation indices: (0) VnGP, (1) APH, (2) CRU, (3) GPCC, (4) UDEL, (5) CPC. [Colour figure can be viewed at wileyonlinelibrary.com].

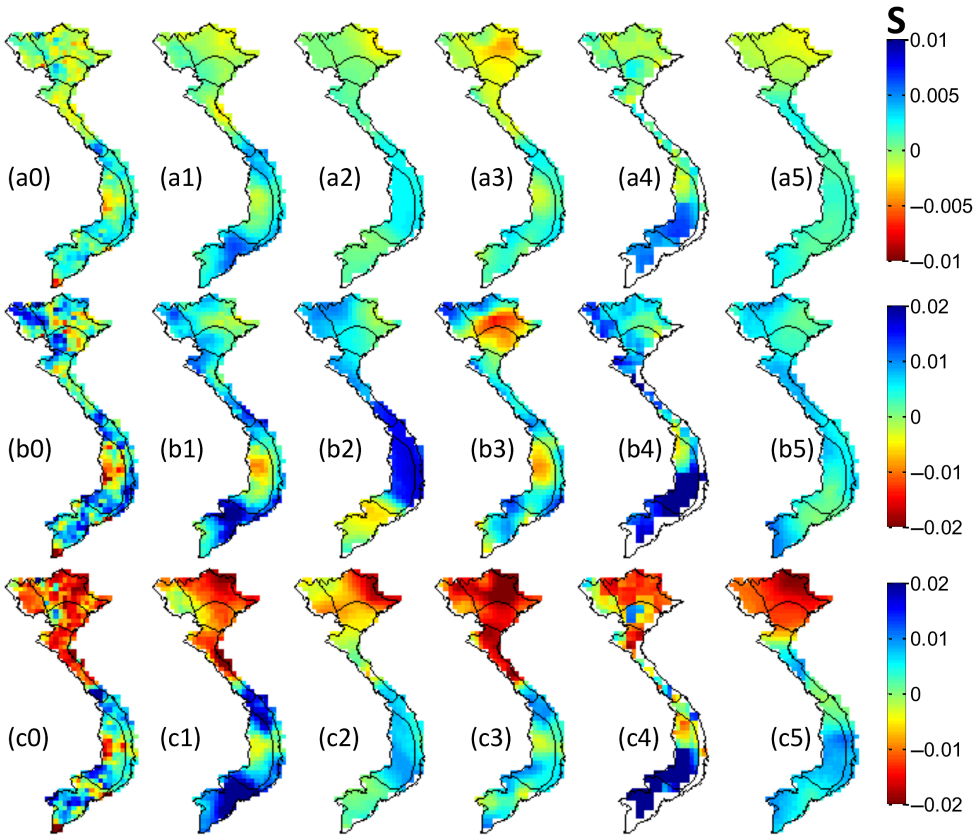


Figure 13. Sen's slopes magnitude for SPI 6 trend analysis: (a) annual (unit: SPI 6/annum), (b) SW monsoon (JJA) (SPI 6/3 months), (c) NE monsoon (DJF) (SPI 6/3 months). Notation indices: (0) VnGP, (1) APH, (2) CRU, (3) GPCC, (4) UDEL, (5) CPC. [Colour figure can be viewed at wileyonlinelibrary.com].

 

were evaluated. While all models (except UDEL) were able to exhibit the characteristics of percentage of drought/wetness events and severity, however, large uncertainty was observed in reproducing mean inter-arrival time in most of the data sets except GPCC and APH. Analysis of spatio-temporal wet/dry spell characteristics indicates GPCC as the best data set as compared to the observed information. This may be due to GPCC has the largest collection of ground truth stations over Vietnam as compared to other gridded data. The second best data APH, although having the higher density for the ground truth stations (number of stations per grid cell) over several parts of Vietnam but it has less spatial coverage as compared to GPCC, especially for the coastal area.

- Trend analyses were performed to evaluate the comparative performance of gridded data sets for annual and seasonal time scales. Most of the gridded data sets were able to capture the significant increasing/decreasing trend as well as the change in magnitude for certain regions as compared to observation. Both GPCC and APH are the two best data sets in representing the SPI trend. On the other hand, despite the relatively poor performance of UDEL in capturing SPI and precipitation statistics information, it has the ability to represent the trend test as compared to observation.

## Acknowledgements

We appreciate the suggestions provided by Associate Editor Prof. McKendry and three anonymous reviewers who helped us to improve the quality of our manuscript. We would also thank the research group led by Prof. Phan Van Tan at the Department of Meteorology and Climate Change, Vietnam National University for sharing the Vietnam gridded precipitation data set. We have no conflict of interest to report.

## References

Becker A, Finger P, Meyer-Christoffer A, Rudolf B, Schamm K, Schneider U, Ziese M. 2013. A description of the global land-surface precipitation data products of the Global Precipitation Climatology Centre with sample applications including centennial (trend) analysis from 1901-present. *Earth Syst. Sci. Data* **5**: 71–99.

Birsan MV, Molnar P, Burlando P, Pfaundler M. 2005. Streamflow trends in Switzerland. *J. Hydrol.* **314**: 312–329.

Chen M, Xie P, Janowiak JE, Arkin PA. 2002. Global land precipitation: a 50-yr monthly analysis based on gauge observations. *J. Hydrometeorol.* **3**: 249–266.

Chou C, Chiang JCH, Lan C-W, Chung C-H, Liao Y-C, Lee CJ. 2013. Increase in the range between wet and dry season precipitation. *Nat. Geosci. Lett.* **6**: 263–267. https://doi.org/10.1038/NGEO1744.

Ciais P, Reichstein M, Viovy N, Granier A, Ogee J, Allard V, Aubinet M, Buchmann N, Bernhofer C, Carrara A, Chevallier F, De Noblet N, Friend AD, Friedlingstein P, Grunwald T, Heinesch B, Keronen P, Knohl A, Krinner G, Loustau D, Manca G, Matteucci G, Miglietta F, Ourcival JM, Papale D, Pilegaard K, Rambal S, Seufert G, Soussana JF, Sanz MJ, Schulze ED, Vesala T, Valentini R. 2005. Europe-wide reduction in primary productivity caused by the heat and drought in 2003. *Nature* **437**: 529–533.

Douglas EM, Vogel RM, Kroll CN. 2000. Trends in floods and low flows in the United States: impact of spatial correlation. *J. Hydrol.* **240**: 90–105.

Gandin LS. 1965. Objective analysis of meteorological fields. *Q. J. R. Meteorol. Soc.* **92**(393): 447.

Gocic M, Trajovic SP. 2013. Analysis of precipitation and drought data in Serbia over the period 1980–2010. *J. Hydrol.* **494**(3–4): 32–42.

Guttman NB. 1999. Accepting the Standardized Precipitation Index: a calculation algorithm. *J. Am. Water Res. Assess.* **35**(2): 311–322.

Hamed KH, Rao AR. 1998. A modified Mann–Kendall trend test for autocorrelated data. *J. Hydrol.* **204**: 182–196.

Harris I, Jones PD, Osborn TJ, Lister DH. 2014. Updated high-resolution grids of monthly climatic observations – the CRU TS3.10 dataset. *Int. J. Climatol.* **25**(3): 623–642.

Heim RR Jr. 2002. A review of twentieth-century drought indices used in the United States. *Bull. Am. Meteorol. Soc.* **83**: 1149–1165.

Ho TMH, Phan VT, Le NQ, Nguyen QT. 2011. Extreme climatic events over Vietnam from observational data and RegCM3 projections. *Clim. Res.* **49**: 87–100.

Jones P, Moberg A. 2003. Hemispheric and large-scale surface air temperature variations: an extensive revision and an update to 2001. *J. Clim.* **16**: 206–223.

Legates D, Willmott C. 1990. Mean seasonal and spatial variability in global surface air temperature. *Theor. Appl. Climatol.* **41**: 11–21.

McKee TB, Doesken NJ, Kleist J. 1993. The relationship of drought frequency and duration to time scales. In *Proceeding of 8th Conference on Applied Climatlogy*, American Meteorological Society, Boston, MA, 179–184.

Mishra AK, Coulibaly P. 2009. Developments in hydrometric network design: a review. *Rev. Geophys.* **47**: RG2001. https://doi.org/10.1029/2007RG000243.

Mishra AK, Desai VR. 2005a. Drought forecasting using stochastic models. *J. Stochastic Environ. Res. Risk. Assess.* **19**: 326–339.

Mishra AK, Desai VR. 2005b. Spatial and temporal drought analysis in the Kansabati River basin, India. *Int. J. River Basin Manage.* **3**(1): 31–41.

Mishra AK, Singh VP. 2010. A review of drought concept. *J. Hydrol.* **391**(1–2): 202–216.

Mishra AK, Özger M, Singh VP. 2009. Trend and persistence of precipitation under climate change scenarios. *Hydrol. Proc.* **23**(16): 2345–2357.

Mishra AK, Singh VP, Özger M. 2010. Seasonal streamflow extremes in Texas River basins: uncertainty, trends and teleconnections. *J. Geophys. Res. Atmos.* **116**: D08108.

Mitchell TD, Jones PD. 2005. An improved method of constructing a database of monthly climate observations and associated high-resolution grids. *Int. J. Climatol.* **25**: 693–712.

New M, Hulme M, Jones PD. 1990. Representing twentieth-century space-time climate variability. Part 1: development of a 1961–90 mean monthly terrestrial climatology. *J. Clim.* **12**: 829–856.

New M, Hulme M, Jones PD. 2000. Representing twentieth-century space-time climate variability. Part 2: development of 1901–96 monthly grids of terrestrial surface climate. *J. Clim.* **13**: 2217–2238.

Nguyen XT, Ngo DT, Kamimera H, Trinh TL, Matsumoto J, Inoue T, Phan VT. 2016. The Vietnam Gridded Precipitation (VnGP) data set: construction and validation. *SOLA* **12**: 291–296. https://doi.org/10.2151/sola.2016-057.

Novotny EV, Stefan HG. 2007. Stream flow in Minnesota: indicator of climate change. *J. Hydrol.* **334**(3–4): 319–333.

Palmer WC. 1965. Meteorological drought. Office of Climatology Research Paper 45, Weather Bureau, Washington, DC, 58 pp.

Partal T, Kahya E. 2006. Trend analysis in Turkish precipitation data. *Hydrol. Proc.* **20**: 2011–2026.

Paulo AA, Rosa PD, Pereira LS. 2012. Climate trends and behavior of drought indices based on precipitation and evapotranspiration in Portugal. *Nat. Hazards Earth Syst. Sci.* **12**: 1481–1491.

Phan VT, Ngo DT, Ho TMH. 2009. Seasonal and interannual variations of surface climate elements over Vietnam. *Clim. Res.* **40**: 49–60.

Seiler RA, Hayes M, Bressan L. 2002. Using the standardized precipitation index for flood risk monitoring. *Int. J. Climatol.* **22**: 1365–1376.

Sen PK. 1968. Estimates of the regression coefficient based on Kendall's tau. *J. Am. Stat. Assoc.* **63**: 1379–1389.

Shepard D. 1968. A two-dimensional interpolation function for irregularly-spaced data. Paper presented at 23rd National Conference. ACM: New York, NY.

Shukla S, Wood AW. 2008. Use of a standardized runoff index for characterizing hydrologic drought. *Geophys. Res. Lett.* **35**: L02405.

Sternberg T. 2011. Regional drought has a global impact. *Nature* **472**: 169.

Tabari H, Talaee HP. 2011a. Analysis of trends in temperature data in arid and semi-arid regions of Iran. *Glob. Planet. Change* **79**(1–2): 1–10.

 

Tabari H, Talaee HP. 2011b. Temporal variability of precipitation over Iran: 1966–2005. *J. Hydrol.* **396**(3–4): 313–320.

Van Steenbergen N, Willems P. 2014. Uncertainty decomposition and reduction in river flood forecasting: Belgian case study. *J. Flood Risk Manage.* **8**(3): 263–275.

Vicente-Serrano SM, Begueria S, Lopez-Moreno JI. 2010. A multiscalar drought index sensitive to global warming: the Standardized Precipitation Evapotranspiration Index. *J. Clim.* **23**: 1696–1718.

Vicente-Serrano SM, Begueria S, Lorenzo-Lacruz J, Camarero JJ, Lopez-Moreno JI, Azorin-Molina C, Revuelto J, Moran-Tejeda E, Sanchez-Lorenzo A. 2012. Performance of drought indices for ecological, agricultural and hydrological applications. *Earch Interact.* **16**(10): 1–27.

Vicente-Serrano SM, Lopez-Moreno JI, Begueria S, Lorenzo-Lacruz J, Sanchez-Lorenzo A, Garcia-Ruiz JM, Azorin-Molina C, Moran-Tejeda E, Revuelto J, Ricardo T. 2014. Evidence of increasing drought severity caused by temperature rise in southern Europe. *Environ. Res. Lett.* **9**(4): 1–9.

Vu MT, Mishra AK. 2016. Spatial and temporal variability of Standardized Precipitation Index over Indochina Peninsula. *Cuadernos Invest. Geogr.* **42**(1): 221–232.

Vu TH, Ngo DT, Phan VT. 2013. Evolution of meteorological drought characteristics in Vietnam during the 1961–2007 period. *Theor. Appl. Climatol.* **118**(3): 367–375.

Vu MT, Raghavan VS, Pham DM, Liong SY. 2015. Investigating drought over the Central Highland, Vietnam, using regional climate models. *J. Hydrol.* **526**: 265–273.

Wilmott CJ, Rowe CM, Philpot WD. 1985. Small-scale climate maps: a sensitivity analysis of some common assumptions associated with grid-point interpolation and contouring. *Am. Cartogr.* **12**(1): 5–16.

Yatagai A, Kamiguchi K, Arakawa O, Hamada A, Yasutomi N, Kitoh A. 2012. APHRODITE: constructing a long-term daily gridded precipitation dataset for Asia based on a dense network of rain gauges. *Bull. Am. Meteorol. Soc.* **93**: 1401–1415.

Zhang L, Zhou T. 2015. Drought over Asia: a review. *J. Clim.* **28**: 3375–3399.

 